A Robust Hand Pose Estimation Algorithm for Hand Rehabilitation

Francesca Cordella[1], Francesco Di Corato[2], Loredana Zollo[3], and Bruno Siciliano[1]

[1] PRISMA Lab, Department of Electrical Engineering and Information Technology, Università di Napoli Federico II, via Claudio 21, 80125 Napoli, Italy
{francesca.cordella,bruno.siciliano}@unina.it

[2] Research Center "E. Piaggio", Università di Pisa, largo Lucio Lazzarino, 1, 56100 Pisa, Italy
francesco.dicorato@for.unipi.it

[3] Laboratory of Biomedical Robotics and Biomicrosystems, Università Campus Bio-Medico, via Alvaro del Portillo 21, 00128 Roma, Italy
l.zollo@unicampus.it

Abstract. During a rehabilitation session, patient activity should be continuously monitored in order to correct wrong movements and to follow patient improvements. Therefore, the application of human motion tracking techniques to rehabilitation is finding more and more consensus. The aim of this paper is to propose a novel, low-cost method for hand pose estimation by using a monocular motion sensing device and a robust marker-based pose estimation approach based on the Unscented Kalman Filter. The hand kinematics is used to enclose geometrical constraints in the estimation process. The approach is applied for evaluating some significant kinematic parameters necessary for understanding human hand motor improvements during rehabilitation. In particular, the parameters evaluated for the hand fingers are joint positions, angles, Range Of Motion and trajectory. Moreover, the position, orientation and velocity of the wrist are estimated.

Keywords: hand pose estimation, rehabilitation, Unscented Kalman Filter.

1 Introduction

Cerebrovascular diseases, such as stroke, are the third leading cause of death in industrialized countries and the leading cause of permanent disability [1]. This leads to a remarkable demand of healthcare services with consequently increasing public expenses. The aim of neurorehabilitation is to help patient relearn sensori-motor capabilities by exploiting the plasticity of the neuromuscular system: motor patterns are relearned through repeated execution of predefined movements [2]. Patient monitoring is needed to evaluate the quality of the performed movements, modify the therapy if needed, apply corrective actions and assess patient performance. Systems for human movement tracking applied to

A. Petrosino, L. Maddalena, P. Pala (Eds.): ICIAP 2013 Workshops, LNCS 8158, pp. 1–10, 2013.

rehabilitation [3] are usually divided into two categories: non-visual tracking systems and visual tracking systems. In this paper the attention is focused on systems belonging to the latter class, which are in turn classified as marker-based and marker-less systems. Marker-based motion analysis systems use optoelectronic cameras and reflective markers: although these systems provide an accurate estimation of joints [4], they are expensive and cumbersome. Further, they require a completely structured environment to perform calibration and acquisition. Marker-less systems rely on Computer Vision algorithms that are sensitive to environmental conditions, but usually use one or two cameras making the system cheap and space-saving.

Vision-based techniques for estimating the hand pose are usually grouped into two categories [5]: Model-based and single frame pose estimation. Model-based visual pose estimation consists of finding the best matching between a group of features characterizing the input image and a group of model features. In order to reduce the computational cost of searching, a prediction step is considered. Multiple hypothesis around the prediction are considered to avoid local minima and discontinuities [6] in the matching. In particular, Bayesian filtering techniques using Monte Carlo methods, such as particle filters [7], [8], [9] are applied. Single frame pose estimation does not make assumptions on time coherence, making the problem very hard to solve. Global search over a database of templates [10] and motion constraints [11], [12] are viable solution.

The hand pose estimation approach presented in this paper tries to merge computer-vision and marker-based techniques proposing a cheap system (that facilitates a fundamental step for hand pose estimation: the triangulation process of the visual features) using a monocular camera, with reduced computational cost, easy to implement and robust. It performs the visual analysis of human hand motion and records hand joint kinematics during movements in a robust and repeatable way making the system adapt for home based rehabilitation.

The paper is structured as follows: in Section 2 the hand kinematic model is introduced; in Section 3 the hand pose estimation algorithm is explained; results about the hand pose estimation are presented in Section 4. Finally, conclusions and future work are proposed in Section 5.

1.1 Notation

The exposition relies on a notation very common in the Computer Vision and Robotics community: the generic pose (rotation R_{ij} and translation T_{ij}) of the frame $\mathcal{I}$ with respect to the frame $\mathcal{J}$ is denoted with the group transformation $g_{ij} = \{R_{ij}, T_{ij}\} \in SE(3)$, which maps a vector expressed in the frame $\mathcal{I}$, into a vector expressed in the frame $\mathcal{J}$. $SE(3)$ is the special Euclidean group for the rigid transformations. The notation is simplified for the pose of the wrist frame with respect to a proper fixed reference frame (e.g. the camera frame, $g_{wc} = \{R_{wc}, T_{wc}\}$), for which the subscripts are dropped, for cleaner notation, and it is denoted simply as $g = \{R, T\}$. The inverse transformation is indicated with the notation $g_{ij}^{-1} \triangleq \left\{{R_{ij}}^T, -{R_{ij}}^T T_{ij}\right\} \in SE(3)$. The *action* of the group transformation g_{jk} on g_{ij}, usually denoted with the symbol $\circ$, to indicate function composition, is indicated with a simple product, i.e. $g_{ik} = g_{jk} g_{ij}$, being by definition: $g_{ik} \triangleq \{R_{jk} R_{ij},\, R_{jk} T_{ij} + T_{jk}\}$. The same notation is used for the action of the transformation $g_{jk} \in SE(3)$ on a vector $P_j \in \mathbb{R}^3$, which is indicated as $P_k = g_{jk} P_j$, that is: $P_k \triangleq R_{jk} P_j + T_{jk}$.

2 Hand Kinematic Model

Long fingers are considered as kinematic chains composed of 3 links with 4 Degrees of Freedom (DoFs): 2 DoFs for the MetaCarpo-Phalangeal (MCP) joint and 1 DoF each for the Proximal Inter-Phalangeal (PIP) and Distal Inter-Phalangeal (DIP) joints respectively. It has been assumed a coupling between PIP and DIP joints ($\theta_{DIP} = \frac{2}{3}\theta_{PIP}$) [13]. The thumb is modeled as proposed in [14] with 5 DOFs. The fingers are considered as 5 kinematic chains having the origin in common (i.e. the wrist). Fig. 1 shows the joint reference frames (left) and the Denavit-Hartenberg parameters for the index finger and for the thumb (right). The remaining long-fingers (middle, ring and little) are assumed kinematically equivalent to the index.

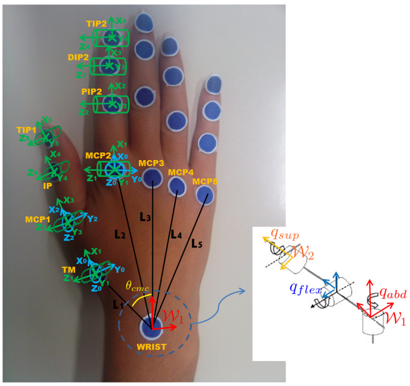

Joint #	a_i	α_i	d_i	θ_i
1	0	-90^o	0	θ^{MCP2}_{abd}
2	L^{index}_P	0^o	0	θ^{MCP2}_{flex}
3	L^{index}_M	0^o	0	θ^{PIP2}
4	L^{index}_D	0	0	θ^{DIP2}

Joint #	a_i	α_i	d_i	θ_i
1	0	-90^o	0	θ^{TM}_{abd}
2	L^{thumb}_P	90^o	0	θ^{TM}_{flex}
3	0	-90^o	0	θ^{MCP1}_{abd}
4	L^{thumb}_M	0^o	0	θ^{MCP1}_{flex}
5	L^{thumb}_D	0^o	0	θ^{IP}

Fig. 1. (left) Protocol used for marker positioning and joint reference frames in the hand starting position. The system reference frame, positioned (in red) on the hand wrist, has the X-axis along the line connecting the marker $WRIST$ with the marker $MCP3$, the Z-axis perpendicular to the palm plane and the Y-axis defined with the right hand rule. (right) DH parameters of the index finger (top) and of the thumb (bottom).

The wrist is modeled as a system with 6 DoFs, consisting of 3 components of translation and 3 angles of rotation (Adduction/Abduction, Flexion/Extension, Pronation/Supination). It is easy to show that these angles correspond to the Euler angles in configuration ZYX. Finally, the palm is assumed to be composed of rigid segments linked to the wrist and its anatomy is assumed known. For the purposes of this work, the arm is supposed not to change its orientation during motion, thus it can be assumed that changes in hand orientation are due to actuation of the wrist joints only. The DH parameters are evaluated in such a way as to obtain a generic algorithm valid for different hand sizes. Therefore, the algorithm envisages an initial calibration phase, where marker centers are detected manually in the first image acquired by the camera and the link lengths are measured, by means of the depth information provided by the vision system. It is assumed that the camera focal axis is perpendicular to the plane where the hand lies.

3 Hand Pose Estimation

3.1 Detection and Tracking

In order to estimate the hand pose, 21 markers, made of blue paper, are placed on the subject hand, as shown in Fig. 1 and a fast detector based on color histogram and a connected component labeling algorithm has been implemented. The Asus Xtion Prolive motion sensing device working at $30fps$ and consisting of an InfraRed (IR) laser emitter, an IR camera for measuring depth information and a RGB camera, with a resolution of 640×480, has been used. The same marker detection algorithm has already been adopted by the authors in a previous work, hence a more detailed explanation can be found in [15]. In the same work, the authors claimed that using simple detection algorithms like the one used may render the task of associating visual measurements to physical markers or deciding whether a given measurement is an outlier or a valid marker projection difficult. For this reason, since a model of the hand is available, the marker tracking problem has been reformulated into a stochastic optimization problem. This renders the proposed algorithm robust with respect to outliers and markers entering and exiting from the field of view.

3.2 Filtering Motion and Pose

The pose parameters – position, $T(t)$ and orientation, $R(t)$ – of the wrist with respect to its initial pose (corresponding to the first image), together with the kinematics of the 17 finger joints can be modeled according to the following discrete-time kinematic model:

$$\begin{cases} T(t+1) = T(t) + v(t)\,dt \\ v(t+1) = v(t) + \eta_v(t)\,dt \\ R(t+1) = R(t)\,e^{(\Omega(t)dt)} \\ \theta_i(t+1) = \theta_i(t) + \eta_{\theta_i}(t)\,dt, \;\; i = 1, \ldots, 17 \end{cases} \tag{1}$$

where $\Omega(t) = \eta_\omega(t)\wedge$, being $\wedge$ the skew-symmetric operator, $\eta_v(t)$, $\eta_\omega(t)$ and $\eta_{\theta_i}(t)$ are zero-mean white noises with constant variance, modeling the hand motions as random walks, and dt is the base sample time, chosen coincident with the sampling rate of the camera. The rotation matrix $R(t)$ is parametrized via Euler angles and encodes the current value of wrist joint angles. The output model is represented by the projection of the visible markers on the image space

$$y_i(t) = \pi\left(g_{w_0c}\,g(t)\,T_{m_iw}(\Theta)\right) + \nu_i(t), \;\; i \in \mathcal{V}(t) \subseteq \{1, 2, ..., 21\} \tag{2}$$

where $\pi() : \mathbb{R}^3 \to \mathbb{RP}^2$ denotes the projective operator, according to the pinhole model, $g(t) = \{R(t), T(t)\} \in SE(3)$ and $T_{m_i w}(\Theta)$ is the $3D$ position of the i-th marker with respect to the wrist reference frame. This position is a function of the hand kinematic parameters Θ, i.e. the joint angles θ_i and the DH parameters, and can be obtained via direct kinematic. The group transformation $g_{w_0 c} \in SE(3)$ is the pose (translation and rotation) between the camera frame and the frame $\mathcal{W}_0$ corresponding to the wrist initial pose, which is assumed known, and $\nu_i(t)$ is a zero-mean white noise with variance R_i, assumed constant among features. A possible algorithm for the iterative estimation of the relative transformation $g_{w_0 c}$ can be found in [16]. The set $\mathcal{V}(t)$ denotes the group of visible markers at the current time (omitting the clutters). It incorporates the time index since the markers may move out of the field of view or be occluded.

According to the kinematic model (1) and the output model (2) a nonlinear estimation scheme has been designed. The aim of the filter is to estimate the state $x(t)$ of the system, consisting of: i) the motion variables, $T(t), v(t)$ and the Euler angles parametrization of the rotation matrix $R(t)$, and ii) the joint angles $\theta_i(t)$ of the fingers. In this paper, given the non linearity of the model with respect to the state and the orientation noise terms, the Augmented Unscented Kalman Filter algorithm presented in [17] has been used. The peculiarity of the adopted estimation scheme, compared with the classical UKF approach [18], is the possibility to easily deal with non-affine noise terms in the state/measurement model. For the remaining part, the technique is a classical UKF as in [18].

3.3 Robust Tracking and Estimation

The challenge in the proposed approach is twofold: above all, using simple detection algorithms like the one described in Sect. 3.1 may render the task of associating a-priori a projection to a physical marker difficult; moreover, the algorithm is desired to be robust with respect to the presence of outliers, occlusions and markers entering and exiting from the field of view.

In [15], the tracking problem has been solved by using Sequential Monte Carlo methods, via adaptation of existing techniques in the framework of multiple target tracking. In that case, the model of the hand has not been available and the markers have been assumed to be independent targets moving on the image plane. On the contrary, the present work takes advantage of the knowledge of the hand model, which allows to constrain the motion of the markers onto the image plane. Thus, the tracking problem is formulated as a stochastic optimization problem embedded into the pose estimation algorithm. The general approach has been presented in [16]. For this aim, the outputs given by the blob detection algorithm, for the image at the time t, are considered a random sequence of M_t measurements $\mathbf{y}_t = \{y_1(t), y_2(t), ..., y_{M_t}(t)\}$ of blob candidates. In general, the condition $M_t \neq 21$ holds, which means that the sequence $\mathbf{y}_t$ does contain projections of visible markers and clutters. The association between measurements and markers/clutters is considered unknown. It is assumed that the sequence $\mathbf{y}_t$ is conditionally independent from every other sequence in the past and that the association of each $y_i(t) \in \mathbf{y}_t$ is conditionally independent from the past history of associations. The filtering problem is thus solved by using a probabilistic technique. To this end, consider a latent variable $a_i(t)$, modeling the measurement-to-marker association:

$$a_i(t) = \begin{cases} 0, & \text{if } y_i(t) \text{ is a clutter} \\ j, & \text{if } y_i(t) \text{ is the projection of marker } j \end{cases} \tag{3}$$

Introducing the latent variable is the same as considering the non linear model (2), in compact form $y(t) = h(x(t))$, as a conditional measurement model over the variable $a_i(t)$. In fact, it is possible to condition the output function over a certain value of the latent variable: i.e. $y_i(t) = h\left(x(t) \middle| a_i(t) = j \neq 0\right)$, with the meaning of selecting the rows corresponding to the projection of the marker j from the function $h(x(t))$. If $a_i(t) = 0$, the output model reduces to $y_i = \nu_o$, $\nu_o \sim \mathcal{N}(\bar{\nu}_o, \Sigma_o)$. It is desired to find the most probable value of the variable $a_i(t)$, $\forall i = 1, \ldots, M_t$, that is for every measurement collected at the current time step. The association problem can be recast as maximizing the belief that the current measurement $y_i(t) \in \mathbf{y}_t$ is either the projection of a visible marker or a clutter. Formalizing, the aim is to find the maximum of the posterior distribution:

$$p\left(a_i(t) \middle| y_i(t), \mathbf{y}_{0:t-1}\right) \propto p\left(y_i(t) \middle| a_i(t), \mathbf{y}_{0:t-1}\right) p(a_i(t)) \tag{4}$$

given the current measurement $y_i(t)$ and the whole history of the measurements up to the previous step. The previous equation has been obtained via application of Bayes' rule. The *prior* $p(a_i(t))$ is determined by the a priori knowledge of clutter and marker association event probabilities [15,16], while the density $p\left(y_i \middle| a_i, \mathbf{y}_{0:t-1}\right)$ is the likelihood that the current measurement is associated to a given marker or to a clutter. This distribution can be obtained via marginalization of a proper joint density:

$$p\left(y_i \middle| a_i, \mathbf{y}_{0:t-1}\right) = \int p\left(y_i \middle| x, a_i, \mathbf{y}_{t-1}\right) p\left(x \middle| a_i, \mathbf{y}_{t-1}\right) dx \tag{5}$$

$$= \int p\left(y_i \middle| x, a_i, \mathbf{y}_{t-1}\right) p\left(x \middle| \mathbf{y}_{t-1}\right) dx \tag{6}$$

where the last equality is obvious since the prediction of the motion parameters of the wrist does not depend on the value of the association for the current measurements set. Fixing a certain guess for the association, $a_i(t) = j,\ j \neq 0$, the density $p\left(y_i \middle| a_i, \mathbf{y}_{0:t-1}\right)$ is the Kalman Filter likelihood of the measurement $y_i(t)$, given the prediction of the marker j, i.e. given the conditioning of the measurement model over *that* value of the latent variable. Thus, given the predicted state-related Sigma-Points [17], $\mathbf{X}^x_{n,t/t-1},\ n = 1, \ldots, L$, computed by employing the nonlinear state model, their transformation through the conditioned measurement function can be obtained, as in the classical UKF:

$$\mathbf{Y}^j_{n,t/t-1} = h\left(\mathbf{X}^x_{n,t/t-1} \middle| a_i = j\right) \tag{7}$$

The superscript j on the transformed Sigma-Points of the output, indicates that $Y^j_{n,t/t-1}$ refers to the predicted projection of the marker j, for which the association is being tested. The mean and covariance of the measurement vector are calculated as:

$$\widehat{y_j^-} = \sum_{n=0}^{L} W_m^n \mathbf{Y}_{n,t/t-1}^j \tag{8}$$

$$P_{yy,j}^- = \sum_{n=0}^{L} W_c^n \left(\mathbf{Y}_{n,t/t-1}^j - \widehat{y_j^-}\right) \left(\mathbf{Y}_{n,t/t-1}^j - \widehat{y_j^-}\right)^T + R_i \tag{9}$$

where W_c^n and W_m^n are the weights associated to the Sigma-Points [17], $\widehat{y_j^-}$ is the predicted projection of the marker j and $P_{yy,j}^-$ its covariance, while R_i is the covariance matrix of the measurements, assumed known. Thus, the probability of the association $a_i = j$ (eq. (6)) can be computed as:

$$p\left(a_i = j \middle| y_i, \mathbf{y}_{0:t-1}\right) \propto \mathcal{N}\left(y_i - \widehat{y_j^-}, P_{yy,j}^-\right) p\left(a_i = j\right) \tag{10}$$

being $\mathcal{N}()$ the multivariate normal distribution of proper mean value and covariance. It is worth to mention that, when testing the association to a clutter, $a_i = 0$, Equation (10) is written as $p\left(a_i = 0 \middle| y_i, \mathbf{y}_{0:t-1}\right) \propto (1/RES)\, p\left(a_i = 0\right)$, where RES is the image resolution, meaning that a clutter can happen everywhere in the image. The set of possible associations is discrete, thus the (discrete) value of the association posterior distribution can be computed by inspecting all the possible values of the associations [16]. Selecting the maximum probability among the ones in equation (10) gives the most probable value of the variable $a_i(t)$, corresponding to the measurement $y_i(t)$. The association problem is solved by repeating the above procedure for all the measurements in the set $\mathbf{y}_t$. Degenerate cases, like multiple associations of different measurements to the same marker and so on, have been considered also, in this work, which solution is detailed in [16]. After the association problem is solved, the correction step can take place, employing the visible markers and the associated image projections, as in the classical UKF.

4 Experimental Validation of Hand Pose Estimation Algorithm

Monitoring human hand joint motion during a rehabilitation session allows extracting quantitative indicators about patient performance. In particular, measure of ROM, A/A and F/E angles of the fingers, wrist orientation and velocity, finger trajectories provide an indication of the ability of a person to perform a movement [19] [20]. The proposed algorithm has been experimentally tested for tracking the whole hand and extracting the above mentioned kinematic parameters during F/E and A/A movements of the fingers and of the wrist and during reach and grasp action. These are standard movements used for understanding the behaviour of each hand joint during a common rehabilitation session. The paper wants to provide a proof-of-concept of the pose estimation approach for evaluating those parameters; hence, the study is still preliminary and is based on

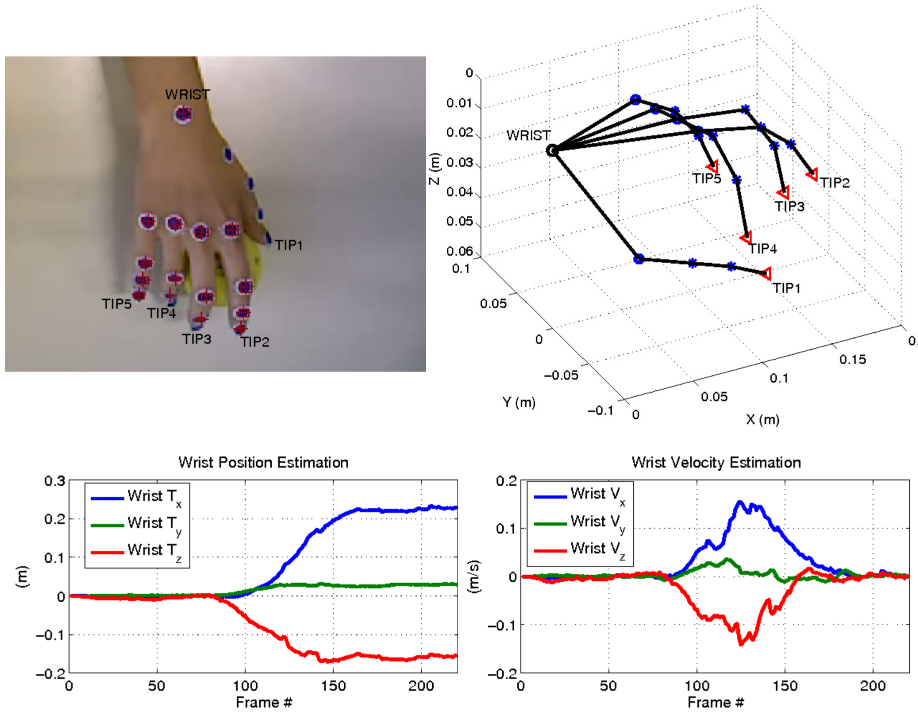

Fig. 2. Pose estimation result (top-right) corresponding to the grasping action of the observed hand (top-left). Position and velocity over time of the wrist during the reaching and grasping phases (bottom). Note that the detector failed with the markers on the thumb due to partial occlusion and shadows, however the pose estimation is still coherent.

the experimental tests on one subject. The participant (a healthy woman of 34 years old) was seated in front of a table with the right hand placed on it. In the starting configuration of the hand, the four fingers are fully extended, the thumb is adducted and the wrist is in a neutral position. The subject was asked to perform reach and grasp actions and finger movements for evaluating joint RoMs paying special attention not to rotate the arm. Fig. 2 shows the final instant of the grasping experiment and the related pose estimation of the hand. Moreover, the acquired data have also been used for analyzing the wrist behaviour in the reaching phase. In particular, Fig. 2, bottom, shows the wrist trajectory and velocity during the reach and grasp action. Fig. 3 shows finger A/A angles and wrist joint angles behaviour. The plotted results are reasonable, in fact it is possible to note that the measured A/A RoMs respect the values of published data on human beings [21]. The previously listed indicators are also extracted but are not reported for the sake of brevity. In conclusion, the approach could be easily used for patient performance evaluation during a rehabilitation session.

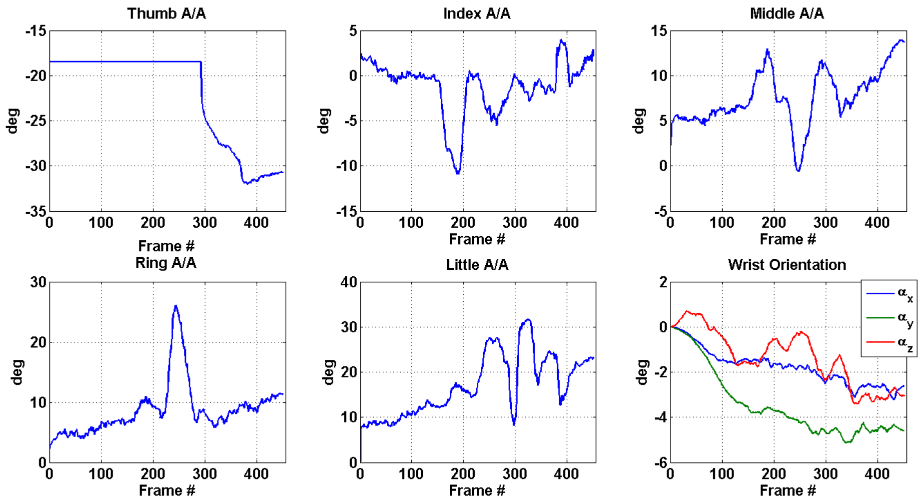

Fig. 3. Fingers A/A motion and wrist angle components during the range of motion experiment

5 Conclusion

In this paper, a novel and low-cost method for hand pose estimation has been proposed. The hand tracking problem has been formulated as a non-linear estimation problem solved by using UKF and considering the interdependence of the markers by introducing the hand kinematic model. Information about the joint orientation, position, trajectory and velocity have been extracted in order to demonstrate that the proposed pose estimation algorithm can be adopted for finding kinematics parameters about the whole hand. The approach can have useful applications in rehabilitation providing quantitative information about the performed task, such as the measurement of joint motion. Further improvements will be devoted to verify the accuracy of the approach by means of a comparison with a ground truth obtained with an optoelectronic system and to test the approach on real patients.

Acknowledgements. This work was supported in part by the National PRIN Project ROCOCÒ – COoperative and COllaborative RObotics (CUP E61J11000300001) and partly by the National PRIN Project HandBot (CUP: B81J12002680008).

References

1. Pellegrino, G., Tomasevic, L., Tombini, M., Assenza, G., Gallotta, E., Sterzi, S., Giacobbe, V., Zollo, L., Guglielmelli, E., Cavallo, G., Vernieri, F., Tecchio, F.: Interhemispheric coupling changes associate with motor improvements after robotic stroke rehabilitation. Restorative Neurology and Neuroscience (2012)

2. Formica, D., Zollo, L., Guglielmelli, E.: Torque-dependent compliance control in the joint space of an operational robotic machine for motor therapy. ASME Journal of Dynamic Systems, Measurement, and Control 128, 152–158 (2006)
3. Zhou, H., Hu, H.: Human motion tracking for rehabilitation–A survey. Biomedical Signal Processing and Control 3, 1–18 (2008)
4. Cerveri, P., De Momi, E., Lopomo, N., Baud-Bovy, G., Barros, R.M., Ferrigno, G.: Finger kinematic modeling and real-time hand motion estimation. Annals of Biomedical Engineering 35, 1989–2002 (2007)
5. Erol, A., Bebis, G., Nicolescu, M., Boyle, R.D., Twombly, X.: A Review on Vision-Based Full DOF Hand Motion Estimation. In: Conf. on Computer Vision and Pattern Recognition, pp. 75–82 (2005)
6. Deutscher, J., Blake, A., Reid, I.: Articulated body motion capture by annealed particle filtering. In: Conf. Computer Vision and Pattern Recognition, vol. 2, pp. 126–133 (2000)
7. Bray, M., Koller-Meier, E., Van Gool, L.: Smart particle filtering for 3D hand tracking. In: Conf. on Automatic Face & Gesture Recognition, pp. 675–680 (2004)
8. Lin, J.Y., Wu, Y., Huang, T.S.: 3D model-based hand tracking using stochastic direct search method. In: Conf. on Automatic Face & Gesture Recognition, pp. 693–698 (2004)
9. Chang, W.Y., Chen, C.S., Hung, Y.P.: Appearance-guided particle filtering for articulated hand tracking. In: Conf. on Computer Vision and Pattern Recognition, vol. 1, pp. 235–242 (2005)
10. Stenger, B., Thayananthan, A., Torr, P.H.S., Cipolla, R.: Hand pose estimation using hierarchical detection. In: Sebe, N., Lew, M., Huang, T.S. (eds.) ECCV/HCI 2004. LNCS, vol. 3058, pp. 105–116. Springer, Heidelberg (2004)
11. Chua, C.S., Guan, H.Y., Ho, Y.K.: Model-based finger posture estimation. In: Asian Conference on Computer Vision (2000)
12. Lee, J., Kunii, T.: Constraint-based hand animation. In: Models and Techniques in Computer Animation, 110–127 (1993)
13. Lin, J., Wu, Y., Huang, T.S.: Modeling the Constraints of Human Hand Motion. In: Proceeding Workshop on Human Motion, pp. 121–126 (2000)
14. Parasuraman, S., Zhen, C.C.S.: Development of Robot Assisted Hand Stroke Rehabilitation System. In: Conf. on Computer and Automation Engineering, pp. 70–74 (2009)
15. Cordella, F., Di Corato, F., Zollo, L., Siciliano, B., van der Smagt, P.: Patient performance evaluation using Kinect and Monte Carlo-Based fnger tracking. In: Conf. on Biomedical Robotics and Biomechatronics, pp. 1967–1972 (2012)
16. Di Corato, F.: A Unified Framework for Constrained Visual-Inertial Navigation with Guaranteed Convergence. PhD Dissertation, University of Pisa (May 2013)
17. Kandepu, R., Foss, B., Imsland, L.: Applying the unscented Kalman filter for nonlinear state estimation. Journal of Process Control 18(7-8), 753–768 (2008)
18. Wan, E.A., Van der Merwe, R.: The unscented Kalman filter for nonlinear estimation. In: Symposium on Adaptive Systems for Signal Processing, Communications, and Control, pp. 153–158 (2000)
19. Zollo, L., Rossini, L., Bravi, M., Magrone, G., Sterzi, S., Guglielmelli, E.: Quantitative evaluation of upper-limb motor control in robot-aided rehabilitation. Medical and Biological Engineering and Computing 9(49), 1131–1144 (2011)
20. Formica, D., Krebs, H.I., Charles, S.K., Zollo, L., Guglielmelli, E., Hogan, N.: Passive wrist joint stiffness estimation. Journal of Neurophysiology (2012)
21. Berger, R.A., Weiss, A.P.C.: Hand surgery (2004)